


## Article

# New Soil Stress Measurement Sensor Based on the Effect of Elastic Charging of Electrodes

Mikhail Kuchumov \* and Sergej Evtushenko 

Department of Information Systems, Technologies and Automation in Construction, Moscow State University of Civil Engineering (MGSU), 129337 Moscow, Russia; evtushenkosi@mgsu.ru

\* Correspondence: mku4umoff@gmail.com

**Abstract:** The purpose of this work was to develop a prototype of a soil stress sensor using a new technique for converting mechanical quantities, with functions for measuring stress changes in soils emerging under the action of a dynamic load associated with earthworks using construction machinery, impact of transport, underground explosions and earthquakes. The development is intended to solve problems in increasing the overall efficiency of monitoring buildings and structures and measurement accuracy. Within the framework of the study, the basic requirements for primary converters of mechanical quantities operating underground were formulated. The design solutions of such sensors, which affect the quality of the information received, have been evaluated. As a result of the study, a new effect of “elastic charging of the interfacial layer of a solid metal electrode” for measuring normal stress in soils was explored and proposed eligible for this purpose. Consequently it became possible to apply this new approach to developing the soil stress measurement sensor, including the creation of its functional scheme of operation, and selection of the hardware set, construction elements and materials taking into account the nature of sensor work. Eventually, laboratory experiments obtaining numerical characteristics were carried out.

**Keywords:** sensor; structural health monitoring; geotechnical monitoring



**Citation:** Kuchumov, M.; Evtushenko, S. New Soil Stress Measurement Sensor Based on the Effect of Elastic Charging of Electrodes. *Buildings* **2022**, *12*, 327. <https://doi.org/10.3390/buildings12030327>

Academic Editors: Giuseppe Lacidogna, Sanichiro Yoshida, Guang-Liang Feng, Jie Xu, Alessandro Grazzini and Gianfranco Piana

Received: 25 January 2022

Accepted: 6 March 2022

Published: 9 March 2022

**Publisher's Note:** MDPI stays neutral with regard to jurisdictional claims in published maps and institutional affiliations.



**Copyright:** © 2022 by the authors. Licensee MDPI, Basel, Switzerland. This article is an open access article distributed under the terms and conditions of the Creative Commons Attribution (CC BY) license (<https://creativecommons.org/licenses/by/4.0/>).

## 1. Introduction

Under the influence of external forces, as well as from their own weight in soils, which are natural multicomponent dynamic systems, stresses and deformations arise, the study of which is currently necessary to solve a number of complex but urgent technical problems.

An incorrect assessment of the building qualities of soils very often leads to the adoption of incorrect organizational and technical decisions at the stage of both projects and economic planning, and in the process of construction and operation, which will certainly affect the cost and timing of certain construction works and, moreover, increases the risk of emergencies posing a danger to human life and health. Analysis [1] of the results of long-term observations of the behavior of buildings and structures, during the construction of which typical errors were made in terms of assessing the characteristics of the soil base and predicting its behavior together with the building, allows us to formulate a number of tasks concerning the need for complex technical monitoring using automated measuring instruments when constructing or operating buildings in difficult geological conditions.

In addition to the practical application of knowledge about the behavior of soils in interaction with man-made technical systems, at the moment many engineering problems arise in experimental and theoretical scientific fields. One of the priority tasks is improving and experimentally substantiating methods for calculating the stress-strain state of foundation structures and modeling their behavior at large ranges of stress changes in the soil (up to 3 MPa) [2], which can help reduce the likelihood of accidents in buildings and structures and violations of their serviceability. Such high stress values in the soil were observed, for example, under the foundation of the reactor compartment of the Zaporozhskaya Nuclear Power Plant during experimental studies under its construction [3].

Recently, great efforts have been made in the study of underground explosions and their effect on buildings and structures, as well as their soil base, since such man-made emergencies are very dangerous, can have an extremely high destructive potential and are accompanied by the risk of accidents, including with lethal outcomes. For example, according to Rostekhnadzor data, almost two thirds of all emergencies, including explosions, at hazardous production facilities in the oil and gas industry are caused by technical factors [4]. Consequently, it is necessary to pay increased attention to improving the methods of monitoring and predicting the geotechnical conditions of the environment under the influence of short-term dynamic loads of an emergency nature.

While studies of the negative effects of dynamic loads caused by seismic activity or explosions on the overground parts of buildings and structures are currently quite comprehensive, experimental data on underground structures and subsoil are extremely scarce [5]. At the same time, this problem lies not only in an insufficient volume of experimental research, but also in terms of mathematical analysis and reliable modeling of soil parameters, which does not allow us to fully see the picture of the behavior of the environment under the influence of high dynamic loads and deformations. This problem is confirmed by the most recent studies on this topic [6], reporting a fairly large difference between the conclusions based on the results of mathematical analysis and the data obtained experimentally.

Based on the foregoing, we can conclude that the issue of improving methods for monitoring the technical condition of buildings and structures is one of the first points in the system of integrated safety of the functioning of construction objects.

For these purposes, a new device is proposed that is installed in the active zone of the soil, below the point of application of the dynamic load and perpendicular to the direction of stress distribution to measure the relative value of these stresses.

## 2. Review of Analogues

At present, the most widely used devices to register normal stress in soil are load cells, which are laid in the active zone of the soil mass at a certain depth, contacting their sensitive elements with soil particles, pore water and gas.

Due to the complexity of determining the stress state of the soil for solving engineering problems, it is assumed that the normal or tangential stresses in any area are equal to the average integral value of the projection of the true stresses, respectively, on the normal or tangential stress to this area. The average integral values of stresses correlate with the strength and deformation properties of soils with a sufficient degree of accuracy and reliability, and therefore fully meet the requirements of engineering problems [7].

It should be noted that load cells cannot directly measure stresses—they capture the deformations of the geological environment in which they are installed. The measured strains are interpreted using various transformations corresponding to the model of the environment under study as stresses.

To measure pressure and mechanical stress, including in geological environments, the most widely used systems are load cells with strain gauges of various designs.

The work of a strain gauge is based on the phenomenon of the strain effect, which consists in a change in the electrical resistance of metals and semiconductors under the influence of mechanical deformations. When measuring mechanical quantities using strain gauges, the primary transducers are sensitive elements that convert the measured mechanical value into deformation of an elastic element, which, in turn, is perceived by strain gauges glued to them.

The sensitivity of a strain gauge to deformations is characterized by the ratio of the change in its resistance under the action of deformation to the value of the relative deformation [8]. This ratio is provided for by the coefficient of relative tensosensitivity  $k$ , determined by the formula:

$$k = \frac{\varepsilon_R}{\varepsilon_l} = \frac{\Delta R/R}{\Delta l/l} \quad (1)$$

where  $\varepsilon_R$ —the relative change in electrical resistance, Ohm;  $\varepsilon_l$ —the relative change in the length of the conductor;  $R$ —electrical resistance, Ohm;  $\Delta R$ —change of electrical resistance, Ohm;  $l$ —conductor length, mm;  $\Delta l$ —change of conductor length, mm.

Taking into account that the electrical resistance of the conductor is related to the specific electrical resistance of the material  $\rho$  and its cross-sectional area  $S_q$ , we transform the formula (1) to determine the coefficient of relative tensosensitivity to the following form:

$$k = 1 + 2\nu + \frac{\Delta\rho/\rho}{\Delta l/l} \quad (2)$$

where  $\nu$ —Poisson's ratio;  $\rho$ —the specific electrical resistance of the material, Ohm  $\times$  m;  $l$ —conductor length, mm.

At the same time, it is necessary to consider the mechanical stress arising in the investigated body  $\sigma$ , determined by the formula:

$$\sigma = E \frac{\Delta l}{l} \quad (3)$$

where  $E$ —the modulus of elasticity of the material of the investigated body, MPa.

From formulas (1)–(3) it is possible to derive the transformation equation of the strain gauge:

$$\frac{\Delta R}{R} = \frac{k\sigma}{E} \quad (4)$$

Since the value of the relative deformation within the elastic properties of the material does not exceed  $2.5 \times 10^{-3}$ , then at  $k = 0.5 \dots 4$  for metals [9] the relative change in resistance will be  $(1.25 \dots 10) \times 10^{-3}$ , that is, 1%. In this regard, the resistance of the strain gauge must have a high temporal stability and have an insignificant temperature coefficient of resistance.

Sensitive elements of strain gauges can be made in the form of a loop-shaped lattice of thin wire (see Figure 1a) or foil (see Figure 1b) in the form of a single crystal plate made of semiconductor material. The sensing element of strain gauges is usually attached to a base of insulating material using a binder such as polyamide or epoxy resin, which mechanically transfers deformation to the sensing element.

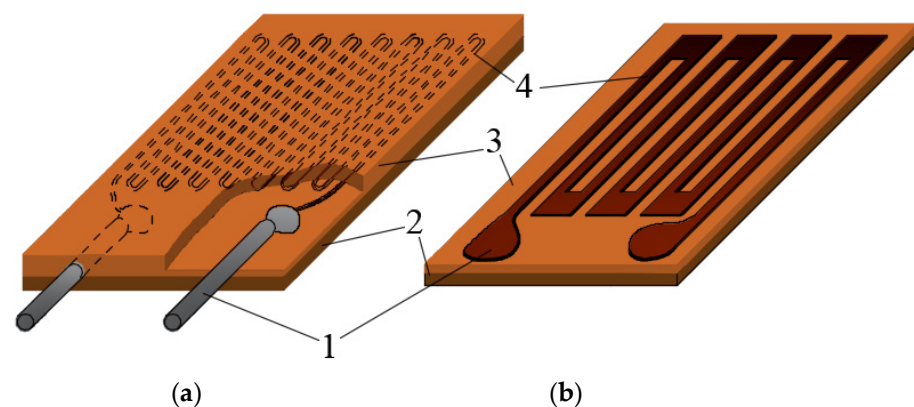


**Figure 1.** Strain gauges: (a)—with a wire sensitive element; (b)—with a foil sensitive element; 1—output contacts; 2—base made of insulating material (substrate); 3—binder (glue); 4—the sensitive element of the strain gauge.

The length of the sensitive element of the strain gauge and its substrate change depending on the temperature; therefore, there is a problem in reducing the temperature sensitivity, which is determined by two physical phenomena: the dependence of the ohmic resistance of the strain gauge material on temperature and the parasitic strain gauge effect,

which arises due to the inconsistency of the temperature expansion coefficients of the strain gauge and the material of the object on which the strain gauge is glued.

The main disadvantages of strain gauges, which prevent their wider introduction, are their one-time use, which does not allow the use of strain gauges after calibration, as well as low sensitivity [10].

Today, strain gauges are used to measure stresses in soil. The main element of such a sensor, which converts the magnitude of the input signal (deformation, pressure from an applied load or stress in the soil) into a signal convenient for measurement, is a flexible elastic element, for example, in the form of a membrane in contact with the ground, or a miniature rod in the form of a beam and acting as a mechanical converter.

The output value of such a sensor is not the stress in the soil mass itself, but the deformation of the elastic element that occurs under the influence of this stress, that is, the measurement is carried out indirectly. From the inner surface of the membrane, a strain gauge is glued to it, which reacts to the deformation (bend) of the membrane.

The “classical” design of the load cell for measuring stresses in the soil is shown in Figure 2. As mentioned earlier, the fixing of the strain gauge to the elastic element is usually carried out using glue, which is an intermediate substance between the investigated body (membrane) and the sensitive element of the strain gauge.

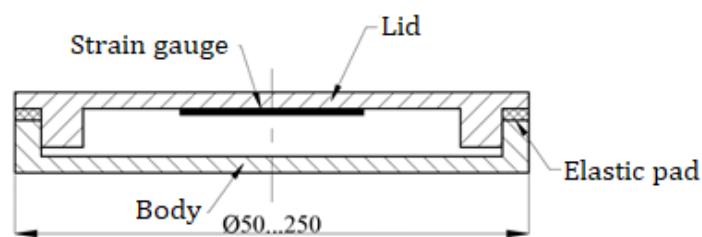


**Figure 2.** The design of the load cell for measuring stresses in the soil.

This feature is the reason for additional errors in glued strain gauges, especially when registering dynamic influences, which ultimately affects the accuracy of the readings.

It is also worth noting that with such a design, the strain gauge will deform only if the adhesive force of the glue affixed to it significantly exceeds the force required to stretch it. At high dynamic and shock loads, the adhesion force between the strain gauge and the adhesive material decreases until the glue layer is completely destroyed and the strain gauge peels off.

It is noted that during the assembly and implementation with various objects and experiments of a large (more than 500) number of mesoscale doses, one of the main reasons for the poor-quality operation of the sensors and their frequent failure was the unsticking of the strain gauge from the sensor body [11]. Thus, it can be concluded that tensoresistive mesos do not fully meet the requirements for reliable and accurate recording of stresses in the soil mass under the action of short-term dynamic loads.

On the Russian market, load cells are presented from various foreign manufacturers, such as: Tokyo Measuring Instruments Laboratory Co. Ltd. (Tokyo, Japan), Earth System S.R.L. (Montechiarugolo, Italy), SISGEO S.R.L. (Masate, Italy), Sungjin Geotec Co. Ltd. (Seoul, Republic of Korea), Ace Instruments (Seoul, Republic of Korea), Xian Chuangjin Electronics Technology Co. Ltd. (Xian, China) and others. Technical characteristics of foreign manufacturers' load cells are summarized in Table 1.

**Table 1.** Technical characteristics of load cells.

Load Cell Model	Diameter, mm	Height (Length), mm	Measurement Range, MPa
Tokyo Measuring Instruments Laboratory Co. Ltd. (Tokyo, Japan)			
KDA-PA	200	25.5	0–2
KDC-PA	100	20.5	0–2
KDE-PA	50	11.3	0–2
Earth System S.R.L. (Montechiarugolo, Italy)			
EPC	200	6	0–2
SISGEO S.R.L. (Masate, Italy)			
L141D	238	13.2	0–10
Xian Chuangjin Electronics Technology Co. Ltd. (Xian, China)			
CJLY-350	28	9	0.05–5
	17	8	0.1–5
Ace Instruments (Seoul, Republic of Korea)			
1910	230	(550)	0–7
1921	150	(182)	0–2

### 3. Sensor Development

#### 3.1. Hardware Determination

The determination of the hardware set of the prototype soil stress sensor was based on the expected characteristics of the output signal, based on the electrochemical principle of the sensor, the nature of the input signal and its operating conditions:

- low amplitude, 2–10 mV;
- high level of periodic interference, 50–200%;
- constant value of the zero-level shift, 1–2 mV;
- negative signal drift over a long period of time (−100  $\mu$ V/hour with continuous measurement, <−10  $\mu$ V/hour at rest).

The location of the sensors and signal processing modules at a significant depth underground provides the basis for predicting a significant reduction in power interference in an operating environment.

Since the electrochemical oxidation/reduction process takes place in the sensor continuously, the potential between the electrodes drops continuously. The rate of fall depends on the rate of internal chemical processes, external load, measurement frequency, and internal parasitic circuits. A decrease in the voltage level between the electrodes from which measurements are taken is called zero drift. Determination of its magnitude and nature of change (time derivative) is a mandatory procedure for post-processing of the measured signal.

The designed system should make autonomous measurements, be located at a short distance from the electrolytic sensor of the load cell, and have its own power source. All this leads to the decision to use a microcontroller as the basis of this system. In this case, the measured signal, after processing and amplification, will arrive and be measured by the built-in analog-to-digital converter (ADC) of the microcontroller.

Standard microcontrollers have two or more ADC channels on board for converting analog signals. Currently, the most popular family of microcontrollers for building energy-efficient measuring systems with support for a large number of third-party software modules (libraries), including open source code—STM32, includes, for example, the STM32F373 microcontroller.

Measuring the signal directly from the microcontroller's ADC cannot provide the required measurement accuracy. The difference is  $0.8 \text{ mV}/100 \text{ } \mu\text{V} = 8$ . Thus, additional conversion (amplification) of the measured signal is indispensable. The voltage amplifier amplifies the input voltage by the required number of times. This factor is called voltage gain and is calculated using the formula:

$$k_u = \frac{U_{out}}{U} \quad (5)$$

where  $k_u$  is the voltage gain;  $U_{out}$ —voltage at the amplifier output, V;  $U$ —voltage at the amplifier input, V.

The output amplified voltage should not depend on the load current and, therefore, on the load resistance. According to the rules, the output resistance  $R_{out}$  should be equal to zero, which is impossible in practice. Therefore, attempts are made to design the voltage amplifier so that  $R_{out}$  is as small as possible.

The minimum gain level that satisfies the accuracy requirements is 8. It should also be borne in mind that degradation of the sensor can lead to an even greater decrease in the zero level of the sensor, which means that the system needs to include the possibility of signal amplification many times greater than 8, for example, 16 or 32.

After elaborating a preliminary technical solution, the following measurement scheme was developed (see Figure 3). The diagram shows the power supply circuits of the electronic control board and the circuits for the formation of reference levels, as well as the input stage of the load resistances. Due to the fact that the source of the measuring signal has a very small amplitude, additional requirements for the input impedance of the measuring path have been introduced into the circuit. At the input, a two-arm resistor bridge circuit with additional resistance along the outgoing wire is assembled.

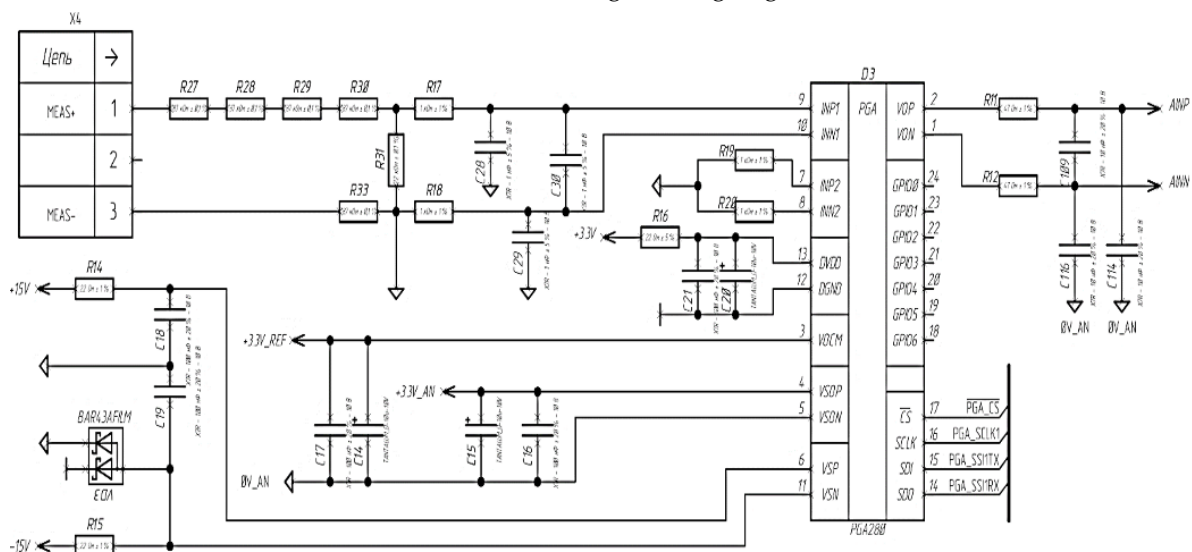


Figure 3. Scheme of electronic control board measurements.

In the upper arm there are four resistors for  $R_1 = 56 \text{ k}\Omega$  each ( $R_{27}, R_{28}, R_{29}, R_{30}$  on the figure) with a confirmed accuracy of at least 0.1%, in the lower (measuring) arm – a resistor  $R_2 = 220 \text{ k}\Omega$  ( $R_{33}$  on the figure) with a confirmed accuracy of at least 0.1%, a resistor  $R_{out}$  is also provided in the outgoing line =  $56 \text{ k}\Omega$  with a confirmed accuracy of at least 0.1%.

According to calculations (see Appendix A) this measurement scheme provides a relative measurement accuracy of 0.156%.

An important aspect in determining the set of sensor hardware is to determine the requirements for a wired communication channel, based on its length and operating conditions underground.



The most negative factor that directly affects the reliability of measurements is electromagnetic interference. Interference is induced in cable circuits through capacitive, inductive and resistive connections. Shielding, twisting and spacing of the supply wires, their proper grounding and good insulation are used to minimize these interferences. The interference signal depends on the length and resistance of the cable conductors, the amplitude and frequency of the noise signal, and also on the relative distance from the cable conductors to the noise source. Since the test leads, which are measured from the prototype ground-stress sensor, will be induced by ambient noise, the distance from the sensor to the signal-processing hardware should be as small as possible.

For a wired communication channel, the RS-485 interface is adopted, due to the high resistance to common mode interference.

### 3.2. Principle of Work

In electrochemistry, it is believed that when a metal electrode contacts an electrolyte solution, a potential jump occurs at the “metal electrode–electrolyte” interface, due to the structure of the electric double layer (EDL). EDL is a thin surface layer of separate electric charges of the opposite sign [12].

As an example, consider what happens when a metal electrode is placed in water (see Figure 4). A layer of positive charges is created by the cores of atoms at the nodes of the crystal lattice (interface), which pass into solution in the form of ions. The layer of negatively charged particles is created by conduction electrons remaining in the electrode.

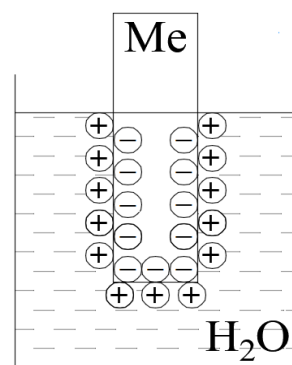


**Figure 4.** EDL system when putting a metal electrode into water.

The phase boundary containing charged particles (ions and electrons) differs in its properties from the volume of the phase. At the interface, transitions of surface particles from one phase to another are possible. As a result of the exchange of charged particles, an excess of electricity carriers of a given sign is created on one side and their deficiency on the other side of the phase boundary. The charge difference at the phase boundary causes a potential jump.

There are two possible cases of capacity formation:

- in the case of using an active metal, a negative potential arises;
- at the same time, a low-active metal leads to the emerging of positive potential.

It should also be noted that the EDL thickness in aqueous solutions does not exceed 2  $\mu\text{m}$ .

In the area of concentrated electrolyte solutions, the EDL system is similar to a flat capacitor, one of the plates of which is formed by charges  $q$  on the surface of a flat metal electrode, and the other by charges of ions of the opposite sign, adjoining from the solution to the electrode surface at a distance  $d$ , equal to the radius of the ion.

The charge density will be proportional to the potential jump between the metal and the solution, and is determined by the following relationship:

$$q = \varphi \cdot c \quad (6)$$

where  $q$  is the charge density, C/cm<sup>2</sup>;  $\varphi$ —potential jump, V;  $c$  is the capacity of the EDL, F. The capacity of a flat capacitor is found by the formula:

$$c = \frac{\varepsilon \cdot S}{4\pi d} \quad (7)$$

where  $S$  is the surface area of the electrode in contact with the electrolyte, cm<sup>2</sup>;  $\varepsilon$  is the dielectric constant of the electrolyte solution, F/cm;  $d$ —radius of the ion, cm.

The principle of operation of a soil stress sensor is that the surface of a metal electrode in contact with an electrolyte increases or decreases by elastic deformation. At the same time, the EDL capacity is attracted according to formula (7), and if the electrode charge is kept constant, for example, by introducing a damping resistance into the electrode circuit, then according to formula (6), the potential of the electrode itself changes relative to the electrolyte solution. The resistance is chosen to be so high that the interfacial layer does not have time to discharge during the deformation period.

The prototype of the soil stress sensor works as follows: when dynamic and quasi-static stresses arise in the soil, they are perceived by the working cover in the form of a steel plate, while the hydraulic fluid deforms the upper elastic metal membrane, and the liquid electrolyte, in turn, transmits the mechanical deformation to the lower elastic metal membrane of the electrochemical cell. It should be noted that with such a functional scheme of work, the stresses in the soil are measured by a direct method, which ensures the highest measurement accuracy.

It is known [12] that if the deformation of the electrode in contact with the electrolyte changes its area, then the “effect of elastic charging” occurs.

One of the main advantages of the sensor based on the “effect of elastic charging of the interphase layer of a solid metal electrode” is the direct transformation of the deformation of an elastic element (electrode of an electrochemical cell) into an electrical signal, which increases the reliability of measurements under dynamic loads rapidly changing in time [13].

### 3.3. Functional Scheme of Work

The soil stress sensor works as follows: when dynamic and quasi-static stresses occur in soils, they are perceived by the working cover in the form of a steel plate, while the hydraulic fluid deforms the upper elastic metal membrane, and the liquid electrolyte, in turn, transfers mechanical deformation to the lower elastic metal membrane of the electrochemical cell. It should be noted that with such a functional scheme of operation, the measurement of stresses in the soil is carried out by a direct method, which ensures the highest measurement accuracy.

A hydraulic transducer was introduced into the functional scheme of the prototype operation (a closed layer of liquid was placed between two membranes of different diameters), which, as known [14], can significantly increase the rigidity of load cells. This design improvement made it possible to increase the rigidity of the sensor without reducing the sensitivity.

The voltage formed on the surfaces of the elastic membrane-electrodes, which is the output signal of the sensor, is transmitted through the contacts brought out of the sensor housing.

The graphic representation of functional scheme of work is shown in Figure 5.



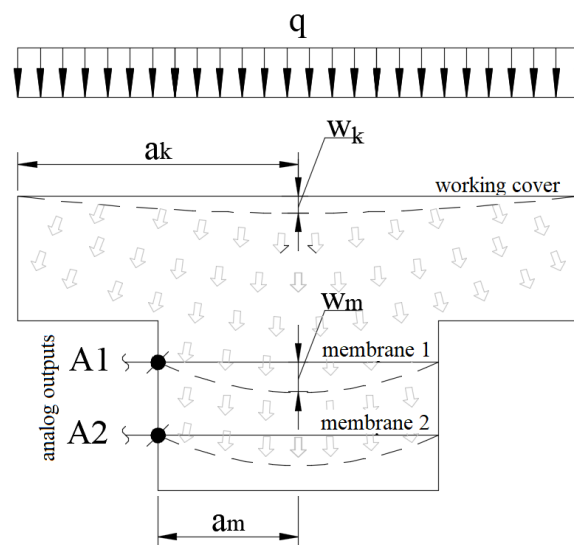


**Figure 5.** Functional scheme of work.

### 3.4. Sensor Construction

The development of a prototype of a soil stress sensor solves the problem of achieving a technical result, which consists in increasing the reliability of measuring stresses in soils due to direct transformation of stresses arising in the soil under the action of external loads.

The prototype of the soil stress sensor consists of a cylindrical steel body with a rigid bottom, which protects the internal structural elements from moisture and soil particles, an electrochemical cell and a working cover, which is a steel plate.

Inside the electrochemical cell made of an electrically insulating material (acrylic), two round elastic metal membranes are rigidly clamped along the contour, which act as electrodes, to which the contacts are soldered outside the sensor body. The membranes are located parallel to each other, and on their inner surfaces, round elastic electrical insulating rubber coatings of half their radius are applied. The presence of a protective coating in this design is dictated by the characteristic of the bending moment arising in the membranes during their deformation under load.

The space between the elastic metal membranes is filled with an electrolyte solution. Between the upper elastic metal membrane of the electrochemical cell and the working cover of the sensor, there is a deaerated hydraulic fluid that transfers mechanical deformations from the medium under study. The tightness of the connection between the working cover and the cylindrical body of the sensor, made with eight screws, is ensured by an elastic annular rubber gasket.

The diagram of the soil stress sensor is shown in Figure 6.

### 3.5. Mathematical Modeling of Working Cover

To determine the calculation scheme, it was assumed that the working cover has a constant thickness, freely supported along the inner contour of the cylindrical body of the sensor, and is loaded with a normal uniformly distributed load over the entire area transferred to the cover by the medium (soil) under study. The operation of the working cover under the action of a load consists in a symmetrical bending. The working cover is assumed to be made of a homogeneous material (metal) with the same mechanical properties in all directions.

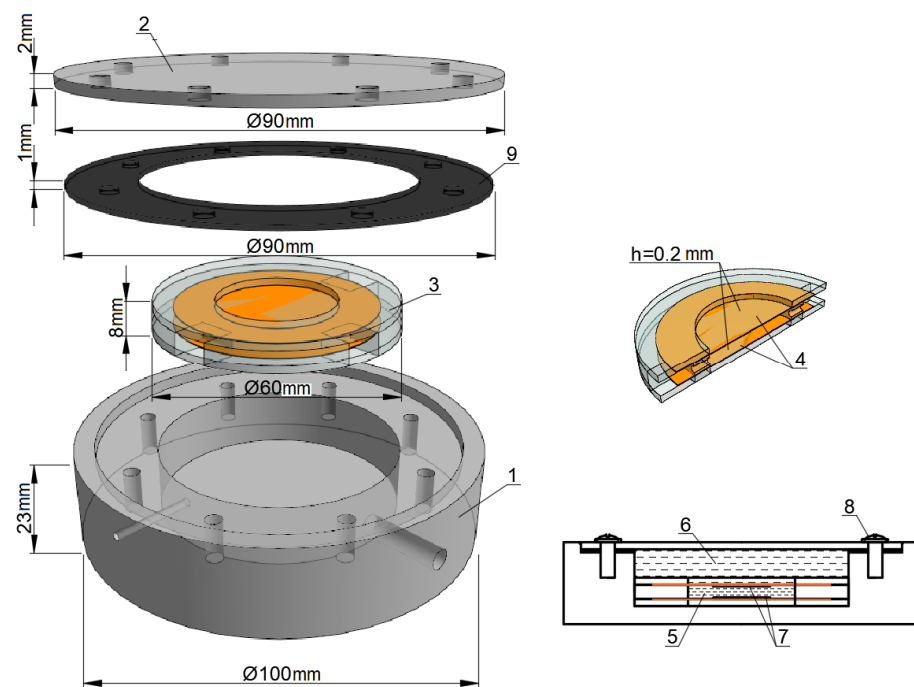


**Figure 6.** Diagram of the device of the soil stress sensor: 1—body; 2—working cover; 3—electrochemical cell; 4—elastic metal membranes; 5—electrolyte; 6—hydraulic fluid; 7—electrical insulating coating; 8—screw; 9—rubber gasket.

The maximum deflection in the center of the working cover ( $w_k > 0$  when directed downwards) with the selected design scheme is determined by the following formula:

$$w_k = \frac{qa_k^4}{64D_k(1+v_k)} \left( 2(1+3v_k)\beta^2 + (3-5v_k)\beta^4 + 8(1+v_k)\beta^2 \ln\beta \right) \quad (8)$$

where  $q$  is the intensity of the external transverse load,  $\text{kg}/\text{cm}^2$ ;  $a_k$  is the radius of the support contour of the working cover,  $\text{cm}$ ;  $D_k$  is the cylindrical stiffness of the working cover material,  $\text{kg}\cdot\text{cm}$ ;  $v_k$  is Poisson's ratio of the material of the working cover;  $\beta$  is the ratio of the radius of the reference contour to the radius of the outer contour.

The intensity of the radial bending moment per unit length of the cylindrical section of the working cover:

$$M_k = \frac{qa_k^2}{16} \cdot \left( 1+3v_k + 2(1-v_k)\beta^2 + 4(1+v_k)\ln\beta \right) \quad (9)$$

The value of the maximum stress that occurs in the working cover under the action of an external transverse load is determined using the formula:

$$\sigma_k = \frac{6M_k}{b^2} \quad (10)$$

where  $b$  is the thickness of the working cover,  $\text{cm}$ .

Expressing the intensity of the external transverse load through the radial moment using formula (9) and assuming the maximum stress equal to the yield strength of the material, we obtain the formula for finding the maximum allowable intensity of the external transverse load on the working cover within the elastic deformation:

$$q_{\max} = \frac{16 \cdot \sigma_{0.2} \cdot b^2}{6a_k^2(1+3v_k + 2(1-v_k)\beta^2 + 4(1+v_k)\ln\beta)} \quad (11)$$

Having found the value of the maximum deflection in the center of the working cover, it becomes possible to determine the volume of hydraulic fluid displaced:

$$V_s = \pi w_k^2 \left( a_k - \frac{1}{3} w_k \right) \quad (12)$$

where  $\pi$  is a mathematical constant.

Using formulas (8)–(12), the working cover of the stress sensor in the soil was calculated for strength and stiffness in various configurations. The material adopted for calculating the working cover is high-quality structural carbon steel according to GOST 1050-88.

The results of the calculation are presented in the form of graphs of the dependence of the maximum allowable intensity of the external transverse load on the working cover (see Figure 7) on various configurations of its overall dimensions (radius— $a$ ; thickness— $b$ ). The red dotted line in the graph indicates the value of the transverse load of 2000 kPa = 2 MPa, which determines the required measurement limit of the stress sensor in the soil.

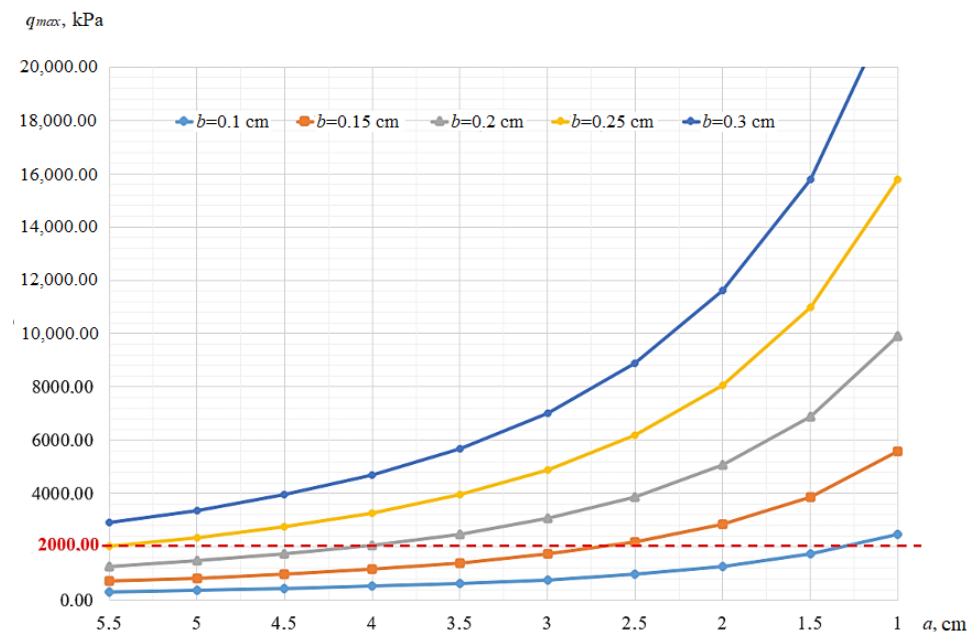


**Figure 7.** Graph of the dependence of the maximum allowable intensity of the external transverse load ( $q_{max}$ ) on the working cover on various configurations of its overall dimensions.

According to the results of the calculation, the most advantageous combination of the overall dimensions of the working cover, with a margin satisfying the conditions for achieving the declared characteristics of the stress sensor in the soil, are accepted to be:

- radius of the reference contour, 3.0 cm;
- outer contour radius, 4.5 cm;
- thickness, 0.2 cm.

### 3.6. Mathematical Modeling of Spring-Sensitive Membrane

To determine the design scheme, it was assumed that the membrane has a constant thickness, rigid clamping along the reference contour in the sensor body excluding angular and linear movements of the fixed edges and is loaded with a normal uniformly distributed load over the entire area.

The work of the diaphragm under load is symmetrical bending. The membrane is assumed to be made of a homogeneous material (metal) with the same mechanical properties in all directions.

The maximum deflection at the center of the membrane ( $w > 0$  in downward direction) is determined by the following formula:

$$w_m = \frac{qa_m^4(1-\rho^2)^2}{64D_m} \quad (13)$$

where  $q$  is the intensity of the external transverse load,  $\text{kg}/\text{cm}^2$ ;  $a_m$ —membrane radius,  $\text{cm}$ ;  $D_m$  is the cylindrical stiffness of the membrane,  $\text{kg}\cdot\text{cm}$ ;  $\nu$ —Poisson's ratio of the membrane material;  $\rho$  is a relative coordinate.

The value of the maximum stress arising in the membrane under the action of an external transverse load is determined using the formula:

$$\sigma_m = \frac{3}{8} \cdot \frac{qa_m^2}{\delta^2} (1 + \nu_m) \quad (14)$$

$\delta$ —membrane thickness,  $\text{cm}$ ;

The intensity of the radial bending moment per unit length of the cylindrical section of the membrane,  $\text{kg}\cdot\text{cm}/\text{cm}$ :

$$M_m = \frac{qa_m^2}{16} \cdot (1 + \nu_m - (3 + \nu_m) \cdot \rho^2) \quad (15)$$

Expressing the intensity of the external transverse load in terms of the radial moment using formula (11) and taking the maximum stress  $\sigma$  equal to the yield stress of the material  $\sigma_{0.2}$ , we obtain the formula for finding the maximum permissible intensity of the external transverse load on the membrane within the elastic deformation:

$$q_{max} = \frac{8 \cdot \sigma_{0.2} \cdot \delta^2}{3a_m^2(1 + \nu_m)} \quad (16)$$

The calculation makes it possible to find the maximum deflection in the center of the membrane, knowing which it is possible to determine the ability of the membrane to perceive the volume of the displaced hydraulic fluid without the occurrence of plastic deformations, which is determined by the satisfaction of the following condition:

$$V = \pi w_m^2 \left( a_m - \frac{1}{3} w_m \right) \geq V_s \quad (17)$$

where  $\pi$  is a mathematical constant;  $V$ —limiting volume of hydraulic fluid perceived by the membrane,  $\text{cm}^3$ ;  $V_s$ —volume of displaced hydraulic fluid,  $\text{cm}^3$ .

To determine the sensitivity of the prototype sensor, the value of the relative deformation of the membrane was determined using the following formula:

$$\varepsilon = \frac{S_1 - S_0}{S_0} \quad (18)$$

where  $S_1$  is the area of the membrane under load,  $\text{cm}^2$ ;  $S_0$ —initial membrane area,  $\text{cm}^2$ .

Since the work of the membrane under load is characterized by symmetric bending, the area of the membrane under load can be found using the formula for determining the area of a spherical segment, taking the maximum deflection in the center of the membrane as the height of the spherical segment:

$$S_1 = 2 \cdot \pi \cdot r_{sph} \cdot w_m \quad (19)$$

where  $r_{sph}$  is the radius of the sphere,  $\text{cm}$ .

Using formulas (13)–(19), the elastic membranes of the stress sensor in the soil were calculated for strength and stiffness in various overall configurations.

The material adopted for the calculation of the membrane is beryllium bronze BrB2 in accordance with GOST 18175-72.

The calculation results are presented in the form of the graphs of the dependence of the maximum deflection in the center of the membranes  $w_m$  (see Figure 8) and relative deformation of membranes  $\varepsilon$  (see Figure 9) on various configurations of their overall dimensions ( $a = 1.0\text{--}5.5\text{ cm}$ ;  $\delta = 0.02\text{--}0.05\text{ cm}$ ).

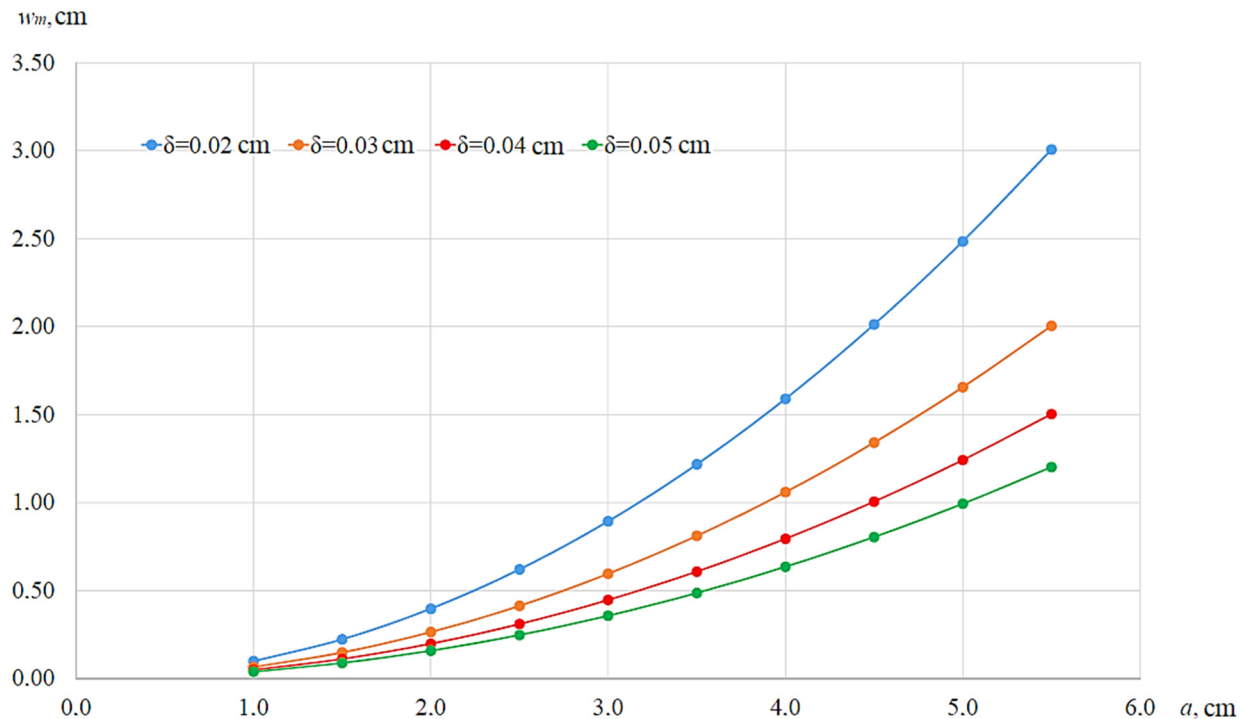


**Figure 8.** Graph of the dependence of the maximum deflection in the center of the membranes ( $w_m$ ) on membrane radius ( $a$ ) and thickness ( $\delta$ ).

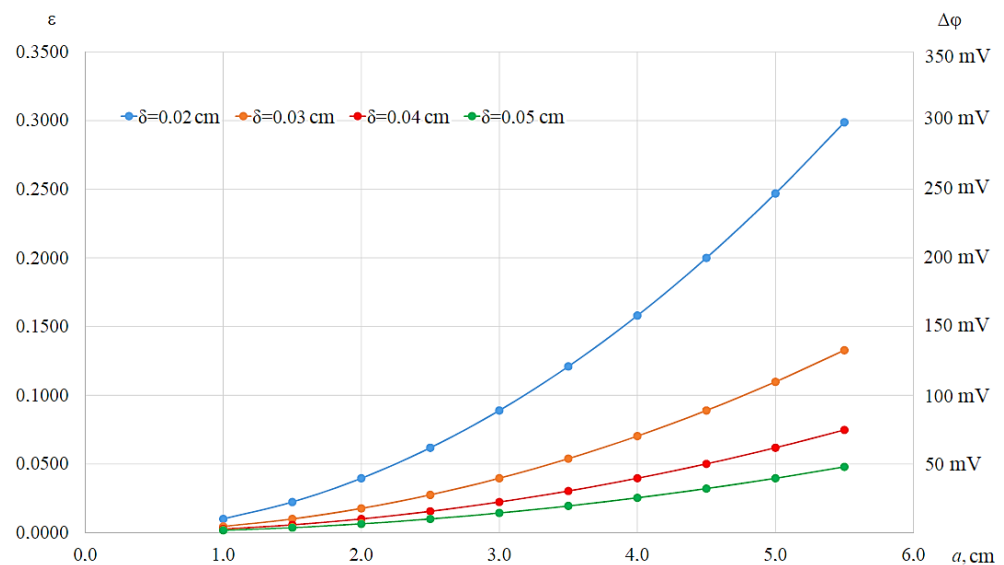


**Figure 9.** Graph of the dependence of the relative deformation of membranes ( $\varepsilon$ ) and corresponding potential jump ( $\Delta\varphi$ ) on membrane radius ( $a$ ) and thickness ( $\delta$ ).

As a result of the calculation, the following diaphragm sizes were chosen:

- radius, 1.5 cm;

- thickness, 0.02 cm.

The selected section of membranes was additionally checked by calculations using the finite element method using the SCAD software package to obtain graphic materials (see Figures 10 and 11). The calculation protocol is presented in the technical documentation of the soil stress sensor prototype.

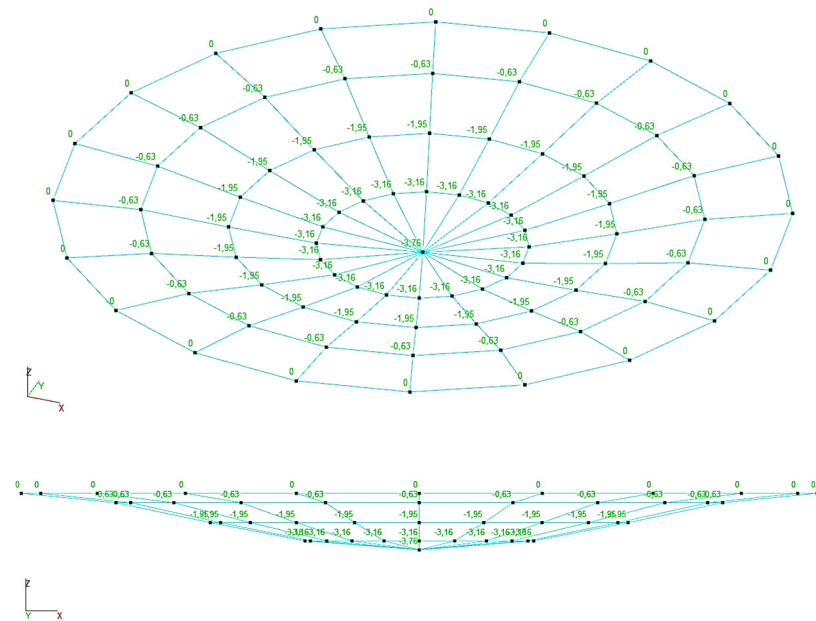


Figure 10. Graphical analysis of displacements in membranes.

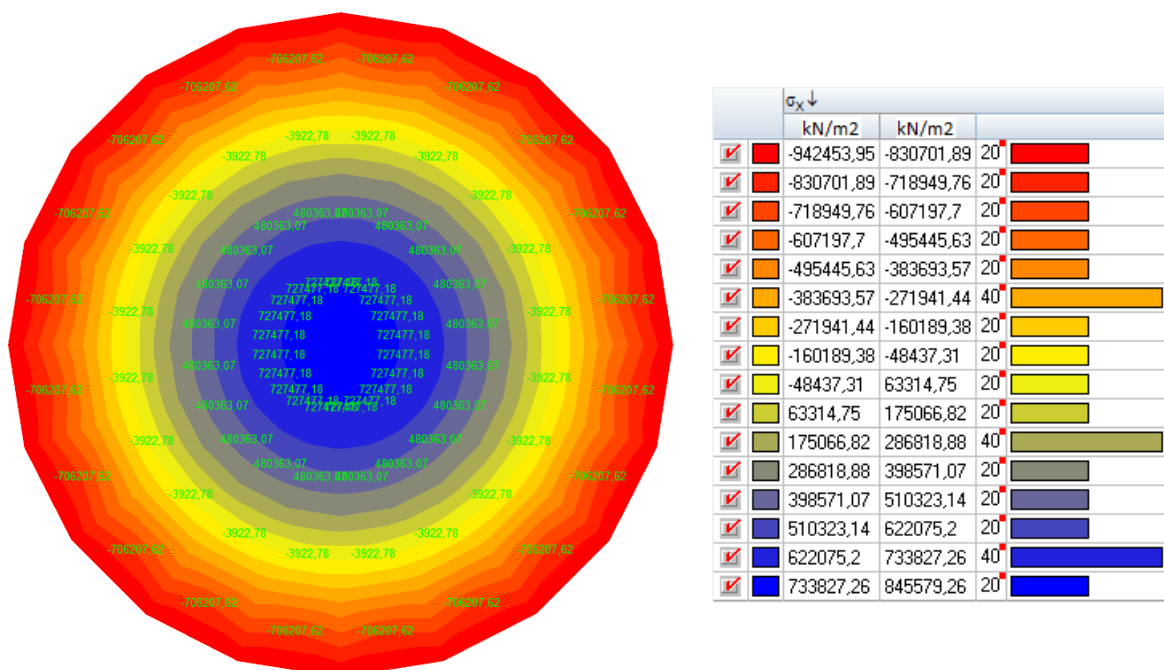


Figure 11. Graphical analysis of stress fields in membranes.

### 3.7. Research of Chemical and Physical Properties

The electrode material in the form of elastic membranes should have good elastic properties under a wide range of external loads and have high corrosion resistance in the selected electrolyte solution.



The electrolyte must have high conductivity and, when paired with the electrode material, maintain stable properties, as well as exhibit the effect of “elastic charging”.

Materials of auxiliary structural elements of the prototype soil stress sensor, which are in direct contact with the electrolyte solution, should not “contaminate” the electrolyte solution and affect its electrochemical properties.

The most important parameters of the materials of elastic elements are the modulus of elasticity and the shear modulus, the values of which should not depend (or depend negligibly little) on temperature, working loads, time and vibrations.

It should be taken into account that for all alloys the modulus of elasticity depends significantly on temperature, and in the general case this dependence is nonlinear. Steel 36NKhTYu and bronze BrB2 have an almost linear dependence of the elastic modulus on temperature in the range from  $-200$  to  $+600$  °C [9].

The maximum value of the converted signal, other things being equal, is determined by the yield strength of the material. The higher the yield point, the greater the permissible value of the converted signal, at which the linear dependence of deformations on the converted forces remains. Relatively high yield strengths for ball-bearing steel ShKh15, structural steel 30KhGSA, steel 36NKhTYu and bronze BrB2 can be seen from the Table 2.

**Table 2.** Physical and mechanical characteristics of some alloys.

Grade	Limit		Modulus		Temperature Coefficient of Linear Expansion, $10^{-6}$ 1/K	Density, mg/m <sup>3</sup>	Application
	Strength Limit, MPa	Yield Point MPa	Elastic Modulus GPa	Shear Modulus, GPa			
Steel ShKh15	2200	1700	210	80	12.0	7.8	Elastic elements of increased accuracy for normal conditions
Steel 36NKhTYu	1127 ... 1225	780 ... 980	176 ... 196	68	12 ... 14	7.9	Elastic elements operating up to 400–500 °C, as well as in aggressive environments
Bronze BrB2	1300 ... 1400	840 ... 1200	128	-	15.8	8.23	Springs and elastic elements of increased speed

One of the most important aspects of the study of the effect of elastic charging of the interphase layer of a solid metal electrode was the selection of an electrolyte solution for the prototype soil stress sensor, carried out on a setup that simulates the elastic tension of a metal electrode under loading. The installation diagram is shown in Figure 12.

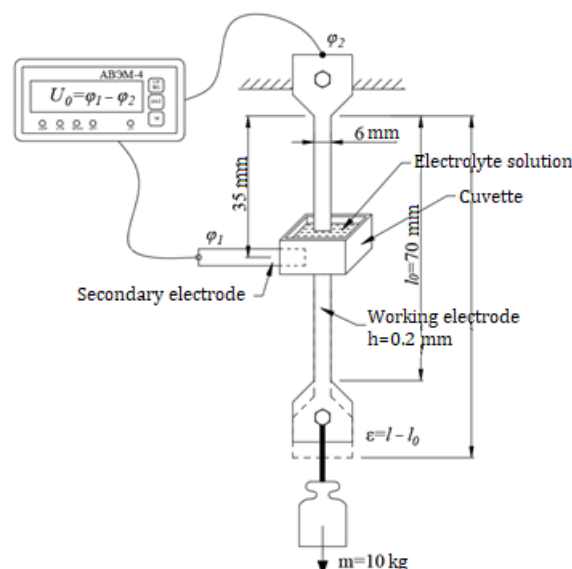


**Figure 12.** Diagram of a pilot plant.

Experimental methodology:

1. the working and auxiliary electrodes were made of BrB2 alloy in the form of strips  $70 \times 6$  mm with a thickness of 0.2 mm, degreased with soda and alcohol, and were not cleaned;
2. technical distilled water and salts (copper sulfate  $\text{CuSO}_4$ , magnesium sulfate  $\text{MgSO}_4$ , sodium chloride  $\text{NaCl}$  and sodium carbonate  $\text{NaHCO}_3$ ) were used to prepare the electrolyte;
3. the electrolyte was not degassed and came into contact with air during the experiment;
4. the electrochemical cell was made of white plasticine;
5. deformation of the working electrode was carried out using a load of  $m = 10$  kg; the application and removal of the load was carried out smoothly, without jerking;
6. the measurements were carried out with an AVEM-4 voltmeter (State Register of SI RF No. 68776-17) of NPP AVEM LLC (Novocherkassk, Russia).

The potential difference between the working and auxiliary electrodes before the application of the load was not equal to zero ( $U_0 \neq 0$ ), which may be associated with chemical processes on their surfaces. After pouring the electrolyte into the cell,  $U_0$  began to change over time—the so-called “zero drift”. In the study, the potential difference during deformation  $U_0^d$  and the potential increment  $\Delta U = |U_0^d| - |U_0|$  were recorded.

#### 4. Manufacturing an Electrochemical Cell

The manufacturing of an electrochemical cell had the following sequence:

- (1) manufacturing of the body of the electrochemical cell, consisting of three ring elements made of plexiglass;
- (2) production of two elastic metal membranes (material—bronze BrB2);
- (3) gluing membranes and ring elements of the body of the electrochemical cell using epoxy resin in two stages with an exposure of 24 h;
- (4) preparation of an electrolyte solution—5% aqueous solution of magnesium sulfate  $\text{MgSO}_4$ ;
- (5) pouring the electrolyte solution into the internal cavity of the electrochemical cell between the metal membranes;
- (6) sealing the filling hole with epoxy resin.

The finished view of the electrochemical cell is shown in Figure 13.



**Figure 13.** Finished view of the electrochemical cell.

During pouring and within 24 h immediately after it, the value of the potential difference resulting from the interaction of the electrolyte solution with electrodes (metal membranes) was recorded. The change in the value of the input signal or “zero drift” immediately after the start of operation of the electrochemical cell was oscillatory in nature with a maximum positive amplitude of 11 mV and a maximum negative amplitude of  $-6.7$  mV. In this case, the highest activity was observed in the first 6 h after electrolyte pouring, and the relative signal stabilization was recorded at the 16th hour after electrolyte pouring. This phenomenon of “zero drift” can be explained by the chemical processes of

oxidation of the surface of metal membranes, which was established earlier at the stage of electrolyte selection.

### 5. Laboratory Test

Tests of the prototype of the stress sensor in the soil were carried out on a calibration unit at the Department of Industrial, Civil Engineering, Geology and Foundation Engineering, South-Russian State Polytechnic University (NPI) named after M.I. Platov. The calibration unit is a thick-walled cylindrical vessel, 430 mm high and 50 mm in diameter, filled with soil, in which a prototype soil stress sensor was installed to a depth of 100 mm (see Figure 14).



**Figure 14.** Calibration unit.

In the lower plane of the vessel lid and over the entire area of its side surface, there is a cavity in the form of a rubber membrane, into which a working medium (water) is pumped under pressure through a hose with shutoff valves, creating a pressure of up to  $25 \text{ kg/cm}^2$  (2.5 MPa). The membrane is in direct contact with the soil and, expanding under pressure, causes stress in the soil inside the vessel.

The preliminary test consisted of stepwise loading of the soil from 0 MPa to 2.0 MPa with continuous recording of the output signal of the sensor prototype with a voltmeter.

According to the results of the preliminary test, graphs of the dependence of the stress in the soil that occurs under load (input signal) on the potential difference (output signal) were obtained:

At a voltage in the ground of 0 MPa, the zero drift without load was  $300 \mu\text{V}$  for 5 min (see Figure 15). It can be seen from the graph that the output signal is characterized by a significant “zero drift” both with and without load, which gives the right to conclude that it is necessary to fix the initial value of the output signal directly at the moment the load is applied, which will be the starting point. This means that the prototype of the soil stress sensor has an incremental, rather than an absolute, nature of operation; in other words, the device is able to reliably record only the change in soil stress, but not its current value.

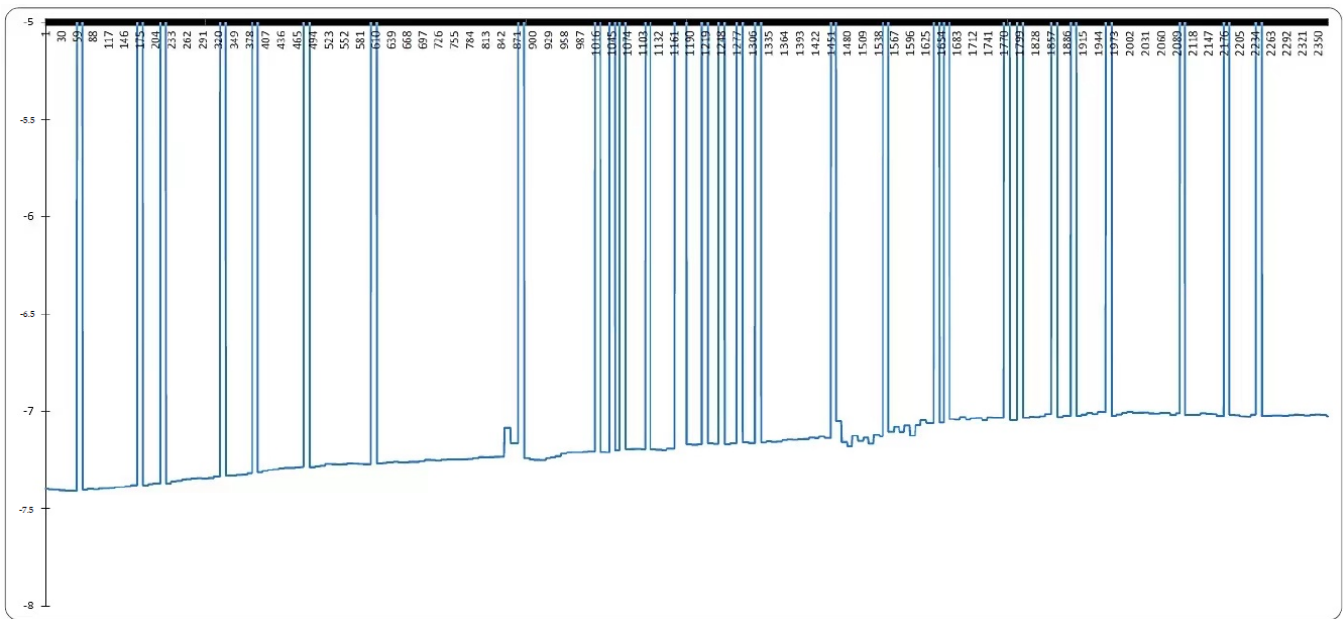


**Figure 15.** Characteristic of the output signal at a stress in the soil of 0 MPa.

During the period of occurrence of stresses in the soil from 0 to 0.75 MPa (see Figure 16), it was not possible to obtain unambiguous data on the appearance of an input signal in the measurement system. Stresses in the range of 0.75–2.0 MPa were recorded with the possibility of their unambiguous interpretation.

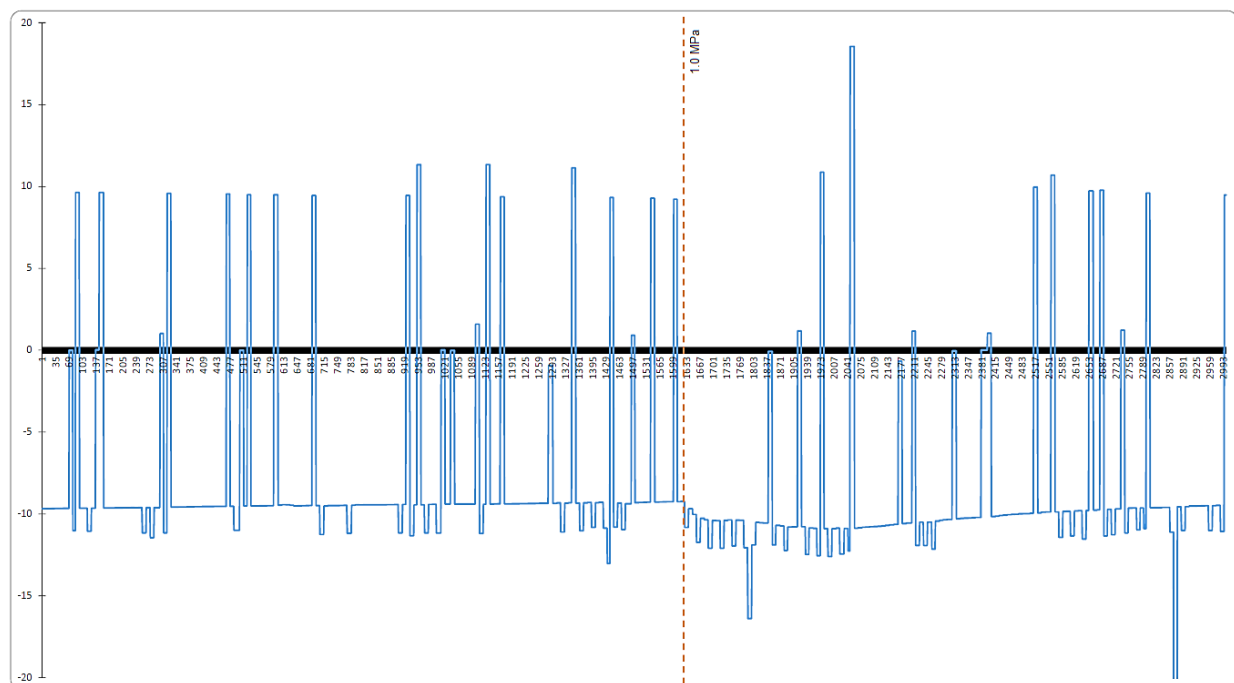


**Figure 16.** Characteristic of the output signal at a stress in the soil of 0–1.0 MPa.

The potential jump with the total stress in the soil  $\sigma = 1.0$  MPa and the incremented stress  $\Delta\sigma = 0.25$  MPa was  $\Delta U = 3.2022$  mV (see Figure 17).

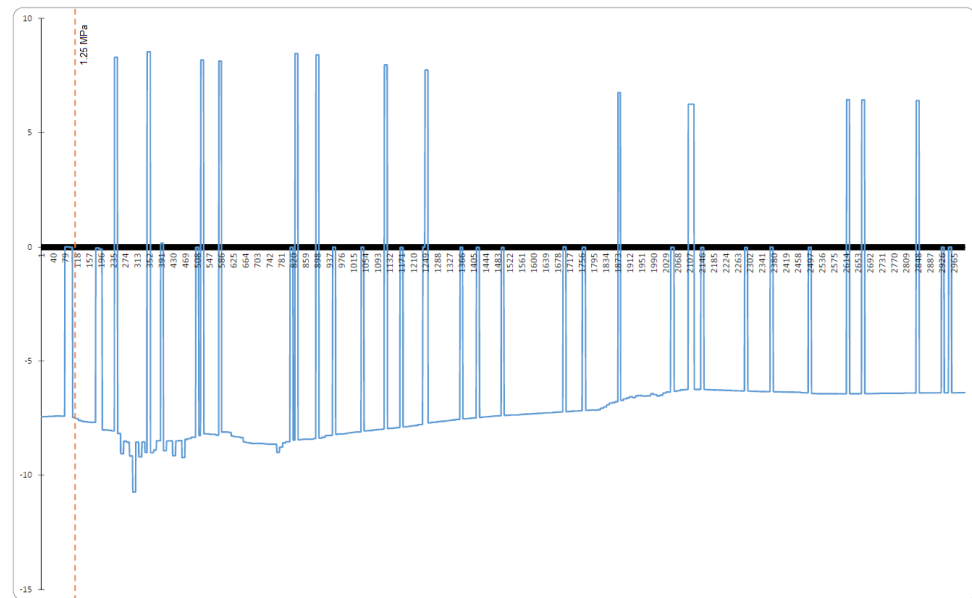


**Figure 17.** Characteristic of the output signal at a stress in the soil of 1.0–1.5 MPa.

The potential jump with the total stress in the soil  $\sigma = 1.25$  MPa and the incremented stress  $\Delta\sigma = 0.25$  MPa was  $\Delta U = 3.1088$  mV.

The potential jump with the total stress in the soil  $\sigma = 1.5$  MPa and the incremented stress  $\Delta\sigma = 0.25$  MPa was  $\Delta U = 3.6264$  mV.

The potential jump with the total stress in the soil  $\sigma = 1.75$  MPa and the incremented stress  $\Delta\sigma = 0.25$  MPa was  $\Delta U = 1.7180$  mV.

The potential jump with the total stress in the soil  $\sigma = 2.0$  MPa and the incremented stress  $\Delta\sigma = 0.25$  MPa was  $\Delta U = 3.2791$  mV.

## 6. Conclusions

- (1) In accordance with the nature of the sensor operation and the expected value of its output signal, a set of hardware was selected and a measuring circuit able to provide a measurement accuracy of 0.156%. was developed.
- (2) According to the results of mathematical modeling, the dimensions of the elastic elements of the sensor were selected:
  - a. radius and thickness of the working cover were selected (radius of the reference contour—3.0 cm; outer contour radius—4.5 cm; thickness—0.2 cm);
  - b. radius and thickness of the spring sensitive membranes were selected (radius—1.5 cm, thickness—0.02 cm);

In addition, the measurement limit of sensor was determined (2.0 kPa) based on the calculations.

- (3) The results of the electrolyte solution selection experiment:
  - a. the output signal was in the range of 0.4–2.1 mV with a load of 10 kg;
  - b. the increase in the potential of the working electrode, deformable under the action of the load, reached the highest value ( $\Delta U = 2.1$  mV) when using a 5% aqueous solution of magnesium sulfate  $\text{MgSO}_4$ ;
  - c. the occurrence of “zero drift” (up to 2.8 mV), which can be explained by the chemical processes of oxidation of the surface of the electrodes, as evidenced by the formation of black plaque, since they border on air and were not completely immersed in the electrolyte solution—this effect should be taken into account in the signal processing from the sensor;

- d. there was a trend towards a decrease in the value of the potential increment in the “loading–unloading” mode with each subsequent load application, which can be explained by the plastic properties of the working electrode material.

Summing up the results of the experiment, it is possible to conclude that the effect of elastic charging of the interphase layer of a solid metal electrode can be used to convert a mechanical quantity into an electrical signal.

#### (4) The results of the laboratory test

The relationship between the total stress in the soil and the value of the output signal has not been established, which once again indicates the incremental, and not the absolute nature of the transformation of the input value.

After the voltage increment in the ground, the output signal returns to its original value over a certain period of time. The potential difference with increasing voltage in the soil can both decrease and increase, which indicates the need to take into account only the numerical value of the electrical signal without taking into account the sign.

**Author Contributions:** Conceptualization, M.K. and S.E.; methodology, S.E.; software, M.K.; validation, M.K. and S.E.; formal analysis, M.K.; investigation, M.K. and S.E.; resources, S.E.; data curation, S.E.; writing—original draft preparation, M.K.; writing—review and editing, S.E.; visualization, M.K.; supervision, S.E.; project administration, S.E.; funding acquisition, M.K. and S.E. All authors have read and agreed to the published version of the manuscript.

**Funding:** Foundation for Assistance to Small Innovative Enterprises in Science and Technology (FASIE).

**Institutional Review Board Statement:** Not applicable.

**Informed Consent Statement:** Not applicable.

**Data Availability Statement:** Not applicable.

**Conflicts of Interest:** The authors declare no conflict of interest.

## Appendix A

The total input impedance is:

$$R_{total} = 4 \cdot R_1 + R_2 + R_{out} \quad (A1)$$

where  $R_1$  is the resistance of the resistors of the upper arm of the electronic control board measurement circuit, kOhm;  $R_2$ —resistance of the resistor of the measuring arm of the electronic control board, kOhm;  $R_{out}$ —resistance of the outgoing line of the electronic control board, kOhm.

$$R_{total} = 4 \times 56 + 220 + 56 = 500 \text{ kOhm}$$

With an input signal  $U = 10 \text{ mV}$  at the resistance of the second arm, the output signal will be:

$$U_{out} = \frac{U}{R_{total}} \cdot R_{out} \quad (A2)$$

where  $U_{out}$  is the voltage at the amplifier output, mV;  $U$ —voltage at the amplifier input, mV.

$$U_{out} = \frac{10}{500} \times 220 = 4.4 \text{ mV}$$

After amplifying the output signal with a factor of 128, the signal at the microcontroller input, determined by transforming the formula (5), will be:

$$U'_{out} = 128 \times 4.4 = 536 \text{ mV}$$



Thus, according to the formula, this will be 15.6% of the entire range that can be measured by a microcontroller—3.6 V. However, with 12-bit accuracy, this gives 641 measurement gradations, which provides a relative measurement accuracy of 0.156%.

## References

1. Evtushenko, S.I.; Kuchumov, M.A. Analysis of the results of long-term observations of building deposits and the state of their bearing structures. In Proceedings of the Materials of the International Scientific and Technical Conference, Novocherkassk, Russia, 29–31 May 2018; pp. 576–580. (In Russian)
2. Ter-Martirosyan, Z.G.; Telichenko, V.I.; Korolev, M.V. *Problems of Soil Mechanics, Foundations and Foundations in the Construction of Multifunctional High-Rise Buildings and Structures*; Bulletin MGSU: Moscow, Russia, 2006; p. 20. (In Russian)
3. Lazebnik, G.E. *Soil Pressure on Structures*; State Research Institute of Building Structures of the Gosstroy of Ukraine: Kyiv, Ukraine, 2005; pp. 158–162. (In Russian)
4. Odnokopylov, G.I.; Sarkisov, D.Y. *Estimation of Parameters of Destroying Load Under Shock Wave for Responsible Building Structures of the Oil and Gas Complex*; Izvestia Tomsk Polytechnic University, ENGINEERING OF GEORESOURCES: Tomsk, Russia, 2017; p. 85. (In Russian)
5. Lu, Y.; Wang, Z.; Chong, K. A comparative study of buried structure in soil subjected to blast load using 2D and 3D numerical simulations. *Soil Dyn. Earthq. Eng.* **2005**, *25*, 275–288. [[CrossRef](#)]
6. Ambrosini, D.; Bibiana, L. Effects of underground explosions on soil and structures. *Undergr. Space* **2020**, *5*, 324–338. [[CrossRef](#)]
7. Golly, A.V. *Method for Measuring Stresses and Strains in Soils*; LISI: Leningrad, Russia, 1984; 53p. (In Russian)
8. Makarov, R.A. *Tensometry in Mechanical Engineering*; Mechanical Engineering: Moscow, Russia, 1975; p. 15. (In Russian)
9. Sharapov, V.M.; Polishchuk, E.S.; Koshevoy, N.D.; Ishanin, G.G.; Minaev, I.G.; Sovlukov, A.S. *Sensors: A Reference Manual*; Technosphere: Moscow, Russia, 2012; pp. 96, 141. (In Russian)
10. Arushonok, Y.Y. *Application of Electrotensometry and Digital Technologies in the Testing of Building Constructions*; Series: Building and Architecture; Bulletin of the Volgograd State University of Architecture and Civil Engineering: Volgograd, Russia, 2021; p. 335. (In Russian)
11. Kulikov, A.V. *Measurement of Stresses in Soils with Modernized Sensors*; Transport Facilities, 2019; p. 4, (In Russian). [[CrossRef](#)]
12. Gokhshtein, A.Y. *Surface Tension of Solids and Absorption*; Publishing House “Science”: Moscow, Russia, 1976; pp. 33, 116–117. (In Russian)
13. Starchy, T.A. New Systems for Monitoring and Controlling Defects and Damages in Building Structures, 2020. *Constr. Archit.* **2020**, *8*, 11–18. (In Russian) [[CrossRef](#)]
14. Baranov, D.S. Selection of the main parameters of soil wells from the conditions of the least distortion of the measured pressures. In *Proceedings of TsNIISK*; Gosstroyizdat: Moscow, Russia, 1962; Volume 14. (In Russian)